ELSEVIER

Microporous and Mesoporous Materials 27 (1999) 207–216

MICROPOROUS AND MESOPOROUS MATERIALS

Novel pathways for the preparation of mesoporous MCM-41 materials: control of porosity and morphology

Michael Grün [a,*], Klaus K. Unger [a], Akihiko Matsumoto [b], Kazuo Tsutsumi [b]

[a] *Institut für Anorganische Chemie und Analytische Chemie, Johannes Gutenberg-Universität, J.J. Becherweg 24, D-55099 Mainz, Germany*

[b] *Department of Materials Science, Toyohashi University of Technology, Tempaku-cho, Toyohashi 441, Japan*

Received 9 February 1998; received in revised form 24 April 1998; accepted 26 April 1998

Abstract

Two novel synthesis routes for the preparation of mesoporous MCM-41 materials are introduced. Both methods use tetra-*n*-alkoxysilanes such as tetraethoxysilane (TEOS) or tetra-*n*-propoxysilane (TPS) as a silica source which are added to an aqueous solution of a cationic surfactant in the presence of ammonia as catalyst. In this study, *n*-alkyltrimethylammonium bromides and *n*-alkylpyridinium chlorides were employed as templates. The addition of an alcohol (e.g. ethanol or isopropanol) leads to a homogeneous system which allows the formation of spherical MCM-41 particles. The main advantages of these methods are short reaction times, excellent reproducibility and easy preparation of large batches.

Keywords: Control; MCM-41; Mesoporous; Morphology; Synthesis

1. Introduction

Since its discovery in 1992 [1,2], MCM-41 has become the most popular member of the M41S family of mesoporous silicate and aluminosilicate materials. The most interesting feature of MCM-41 is its regular pore system which consists of an hexagonal array of unidimensional, hexagonally shaped pores. The pore diameter of MCM-41 can be varied systematically between 2-10 nm [2]. Other interesting physical properties of MCM-41 include a highly specific surface of up to $1500\ m^2\ g^{-1}$, a specific pore volume of up to $1.3\ ml\ g^{-1}$ and a high thermal stability, all of which make it suitable for many catalytic applications. The catalytic properties can be adjusted by incorporation of different metals such as titanium and aluminium into the MCM-41 framework [3–5]. Due to its regular pore structure and pore shape, MCM-41 has attracted considerable interest as a model substance for sorption of various gases and vapours [6,7]. Other metal oxides (e.g. tungsten oxide [8], antimony oxide [8] and titania [9]) with an MCM-41 analogue structure have been synthesized. MCM-41 type materials with a defined morphology are promising selective adsorbents in separation techniques e.g. high performance liquid chromatography (HPLC) and supercritical fluid chromatography (SFC) [10–12]. This communication introduces two novel synthesis routes and describes the aging of MCM-41 under high-pH hydrothermal conditions.

For many applications it is desirable to have a method which allows the preparation of large amounts of high-quality MCM-41 in a short period of time. Our method involves the addition of a

* Corresponding author.

1387-1811/99/$ – see front matter
PII: S1387-1811(98)00255-8

tetra-*n*-alkoxysilane such as tetraethoxysilane or tetra-*n*-propoxysilane to an aqueous solution of the template in the presence of ammonia. After the formation of the silica hydrogel, the template is removed by calcination at 823 K.

The first synthesis takes place in a heterogeneous medium because of the insolubility of the tetra-*n*-alkoxysilane in water and results in irregularly shaped MCM-41 particles. A modification of the well known Stöber reaction [13] for the preparation of non-porous silica spheres allows the reaction to take place in a homogeneous environment, resulting in the formation of spherical MCM-41 particles. Here, a low-boiling alcohol such as ethanol or isopropanol is added as a co-solvent for the tetra-*n*-alkoxysilane to make it soluble in the reaction mixture.

The materials were characterized by X-ray diffraction, nitrogen sorption and scanning electron microscopy. We have chosen to determine the pore size of our sample from X-ray diffraction data and by the Wheeler method, as calculating the pore size from nitrogen sorption data by the BJH (Barrett–Joyner–Halenda) method leads to an underestimation of the pore size. Ravikovitch et al. [14–16] have shown that for MCM-41 materials application of the non-local density functional theory (NLDFT) gives pores sizes which are larger by 1.0 nm than those calculated from the BJH theory.

2. Experimental

2.1. Chemicals

n-Dodecyltrimethylammonium bromide, *n*-tetradecyltrimethylammonium bromide, *n*-hexadecyltrimethylammonium bromide, *n*-hexadecylpyridinium chloride monohydrate and *n*-octadecyltrimethylammonium bromide were purchased from Aldrich, Steinheim, Germany. *n*-Eicosyltrimethylammonium bromide was prepared according to a method given by Colichman [17].

Aqueous ammonia (reagent grade, 25 or 32 wt.%), tetraethoxysilane (TEOS, reagent grade) and absolute ethanol (reagent grade) were given by Merck KGaA, Darmstadt, Germany.

All chemicals were used without further purification, TEOS was distilled in vacuo immediately before use for the preparation of spherical MCM-41 particles. All syntheses were carried out at room temperature (293 K).

2.2. Synthesis of MCM-41 (heterogeneous system)

n-Alkyltrimethylammonium bromides of different alkyl chain lengths from C_{12} to C_{20} were used as template. The template was dissolved in 120 g of deionized water to yield a 0.055 mol l^{-1} solution, and 9.5 g of aqueous ammonia (25 wt.%, 0.14 mol) was added to the solution. While stirring 10 g of tetraethoxysilane (0.05 mol) was added slowly to the surfactant solution over a period of 15 min resulting in a gel with the following molar composition: 1 TEOS:0.152 *n*-alkyltrimethylammonium bromide:2.8 NH_3:141.2 H_2O The mixture was stirred for one hour, then the white precipitate was filtered and washed with 100 ml of deionized water. After drying at 363 K for 12 h, the sample was heated to 823 K (rate:1 K min^{-1}) in air and kept at this temperature for 5 h to remove the template.

2.3. Synthesis of MCM-41 spheres (homogeneous system)

2.5 g of *n*-hexadecyltrimethylammonium bromide (C_{16}TMABr, 0.007 mol) was dissolved in 50 g of deionized water, and 13.2 g of aqueous ammonia (32 wt.%, 0.25 mol) and 60.0 g of absolute ethanol (EtOH, 1.3 mol) were added to the surfactant solution. The solution was stirred for 15 min (250 rpm) and 4.7 g of TEOS (0.022 mol, freshly distilled) was added at one time resulting in a gel with the following molar composition:1 TEOS:0.3 C_{16}TMABr:11 NH_3:144 H_2O:58 EtOH. After stirring for 2 h the white precipitate was filtered and washed with 100 ml of deionized water and 100 ml of methanol. After drying overnight at 363 K, the sample was heated to 823 K (rate:1 K min^{-1}) in air and kept at that temperature for 5 h. *n*-hexadecyltrimethylammonium bromide was substituted by an equimolecular amount of *n*-hexadecylpyridinium chloride monohydrate in an additional experiment.

2.4. Aging of MCM-41 under high-pH hydrothermal conditions

MCM-41 prepared with *n*-hexadecyltrimethylammonium bromide as template was transferred into teflon-lined autoclaves together with the mother liquid and aged for 10 days at 378 K and 433 K,

respectively. The aged samples were filtered and washed with 100 ml of deionized water. After drying at 363 K, the sample was heated to 823 K in air (rate:1 K min^{-1}) and kept at this temperature for 5 h.

3. Characterization

3.1. X-ray diffraction (XRD)

X-ray diffraction (XRD) patterns were recorded on a Seifert TT 3000 diffractometer using Cu K_α radiation of wavelength 0.15405 nm. Diffraction data were recorded between 1 and 25° 2Θ at an interval of 0.01 2Θ. A scanning speed of 0.5° 2Θ per minute was used. (automatic divergence slit system).

3.2. Nitrogen sorption

Adsorption and desorption isotherms of nitrogen were obtained at 77 K either on a Micromeritics ASAP 2010 (Micromeritics Instrument Corporation, Norcross, GA, USA) or on a Quantachrome Autosorb 6B (Quantachrome Corporation, Boynton Beach, FL, USA). The samples were outgassed at 423 K and 1 mPa for 12 h before measurements were performed.

3.3. Scanning electron microscopy

Scanning electron micrographs were recorded using a Zeiss DSM 962 (Zeiss, Oberkochen, Germany). The samples were deposited on a sample holder with an adhesive carbon foil and sputtered with gold.

4. Results and discussion

4.1. Synthesis of MCM-41 (heterogeneous system)

The adsorption and desorption isotherms of nitrogen on each sample show the typical type IV isotherm according to the IUPAC nomenclature for MCM-41 (Fig. 1). At the adsorption branch, the adsorbed amount increased gradually with an increase in relative pressure by multilayer adsorption. A sudden uptake of the adsorbed amount was observed over a narrow range of relative pressure (P/P_0) between 0.3 and 0.4 caused by capillary condensation of nitrogen in the mesopores. The desorption branch of the isotherm coincides with the adsorption branch.

Typical X-ray diffraction patterns of MCM-41 usually show four Bragg peaks indicating the long

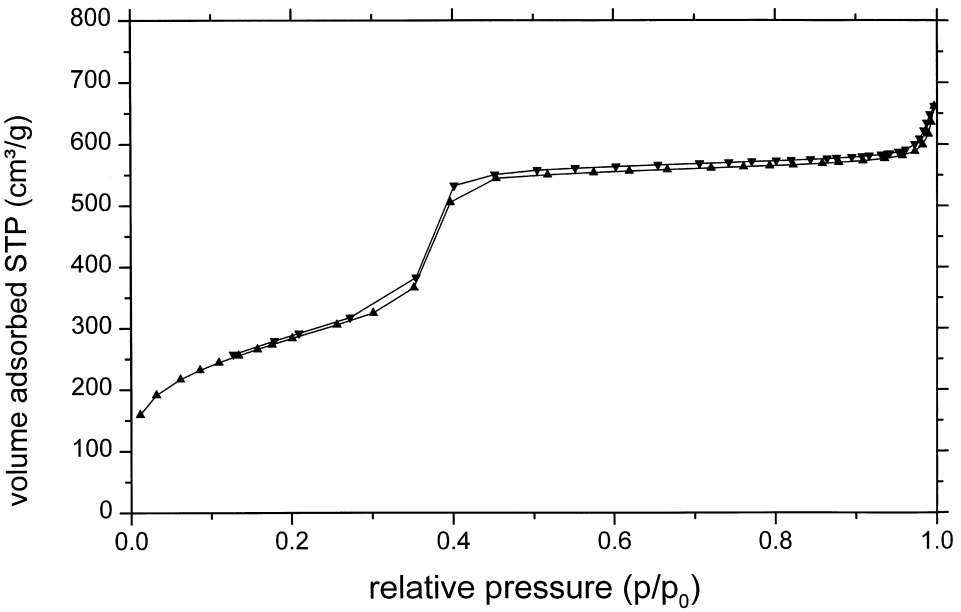

Fig. 1. Nitrogen sorption isotherm of an MCM-41 sample prepared in heterogeneous medium with *n*-hexadecyltrimethylammonium bromide as template (sample no. 3) (▲: adsorption branch, ▼: desorption branch).

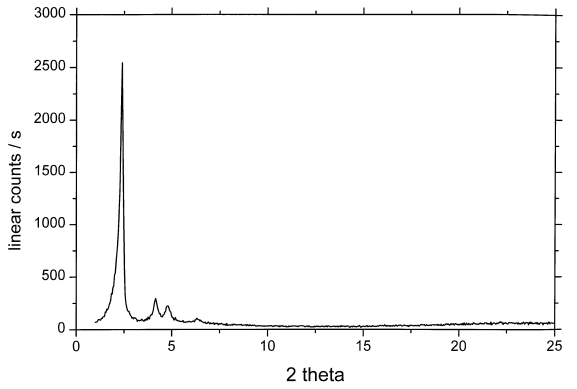

Fig. 2. X-ray diffraction pattern of an MCM-41 sample prepared in heterogeneous medium with *n*-hexadecylpyridinium chloride as template.

range order present in this material, an example of a material prepared with *n*-hexadecylpyridinium chloride is shown in Fig. 2. The Bragg peaks can be indexed assuming a hexagonal symmetry. The repeating distance a_0 between two pore centers may be calculated by $a_0=(2/\sqrt{3})d_{100}$. The pore diameter can be calculated from this value by subtracting 1.0 nm which is an approximate value for the pore wall thickness. The sample prepared with *n*-eicosyltrimethylammonium bromide shows only one broad Bragg diffraction peak.

The properties of the MCM-41 samples prepared by use of different *n*-alkyltrimethylammonium bromides are collected in Table 1. The a_0-value becomes larger with increasing carbon chain length of the alkyl group in the template. The specific surface area gradually decreases from 1450 $m^2\,g^{-1}$ (prepared with *n*-dodecyltrimethylammonium bromide, sample no. 1) to 980 $m^2\,g^{-1}$ (*n*-eicosyltrimethylammonium bromide, sample no. 5) while the values of the specific pore volume increase from 0.63 ml g^{-1} (with *n*-dodecyltrimethylammonium bromide, sample no. 1) up to 1.20 ml g^{-1} (*n*-eicosyltrimethylammonium bromide, sample no. 5) with increasing carbon chain length of the alkyl group in the template. Thus the pore size and the pore volume can be controlled by varying the template. This novel synthesis procedure provides convenient access to high-quality MCM-41 material in a short period of time (10–30 min) without either additional heating or the application of external pressure. These features also make this procedure suitable for the large-batch preparation of MCM-41.

4.2. Synthesis of MCM-41 spheres (homogeneous medium)

The X-ray diffraction patterns of MCM-41 materials [Fig. 3(a) and (b)] prepared in homogeneous medium show several Bragg peaks at low angles between 2.5 and 7.0° 2Θ which are typical of MCM-41 materials. They arise from the quasi-regular arrangement of the mesopores in the bulk material.

Sample 6 (template:*n*-hexadecyltrimethylammonium bromide) exhibits three sharp Bragg peaks, which can be indexed as (100), (110) and (200) in the hexagonal system. [Fig. 3(a)]. A pore diameter of 3.14 nm was calculated using the d_{100} value of 3.6 nm. The diffractogram of sample 7

Table 1
Properties of MCM-41 samples prepared in heterogeneous medium with *n*-alkyltrimethylammonium bromides as templates

Sample no.	Template	Specific surface area[a] ($m^2\,g^{-1}$)	Specific pore volume[b] ml g^{-1})	Pore diameter $4V_p/a_s$ (nm)	Pore diameter (XRD)[c] (nm)
1	C_{12}TMABr	1450	0.63	1.76	2.5
2	C_{14}TMABr	1120	0.74	2.63	2.9
3	C_{16}TMABr	1070	0.85	3.19	3.3
4	C_{18}TMABr	1050	1.09	4.14	3.8
5	C_{20}TMABr	980	1.20	5.04	–[d]

[a] According to the BET equation.
[b] According to the Gurvitch rule.
[c] Using the d_{100}-value and assuming a pore wall thickness of 1.0 nm of sample no. 3.
[d] Very broad X-ray diffraction peak.
V_p: specific pore volume, a_S: specific surface area.

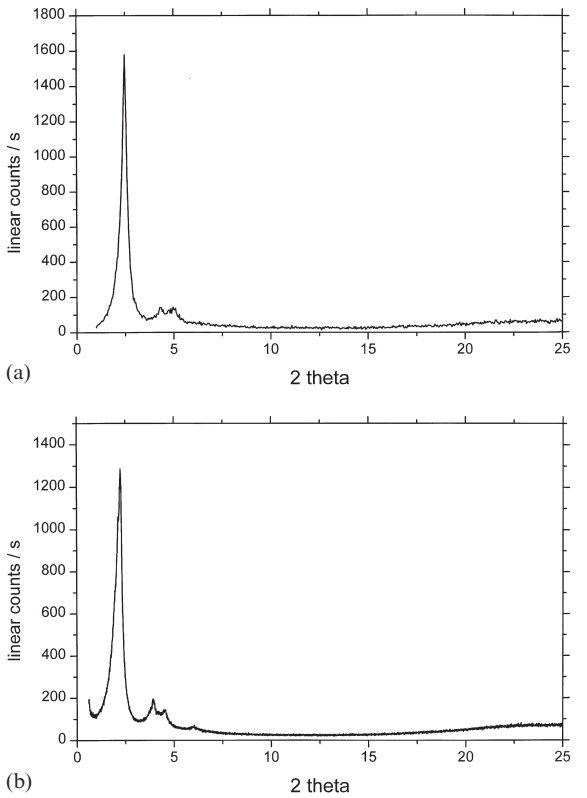

Fig. 3. (a) X-ray diffractogram of MCM-41 spheres, prepared with *n*-hexadecyltrimethylammonium bromide (sample no. 6); (b) X-ray diffractogram of MCM-41 spheres, prepared with *n*-hexadecylpyridinium chloride (sample no. 7).

(template:*n*-hexadecylpyridinium chloride) shows four clearly distinguishable Bragg peaks [Fig. 3(b)]. The fourth peak can be indexed as (210) in the hexagonal system. Calculation of the pore diameter gives a value of 3.05 nm.

The nitrogen isotherms of the investigated materials are shown in Fig. 4(a) and (b). A fairly linear increase of adsorbed volume at low pressures is followed by a steep increase in nitrogen uptake at a relative pressure $P/P_0 = 0.22–0.28$, which is due to capillary condensation inside the mesopores. The long plateau at higher relative pressures indicates that pore filling occurs in a narrow P/P_0 region around a value of 0.25. The isotherm can be classified as a type IV. Both samples show specific surface areas between 1100 and 1220 $m^2 g^{-1}$ and a specific pore volume between 0.8 and 0.95 ml g^{-1}. Application of the BJH method to calculate the pore size distribution is not possible due to the instability of the liquid nitrogen meniscus inside the mesopores which leads to an underestimation of the pore diameter as pointed out before. A summary of all parameters obtained by nitrogen sorption and X-ray diffraction is shown in Table 2.

Scanning electron microscopy was used to determine the particle size, particle morphology and the particle size distribution of the synthesized materials. The particle size of both samples ranges from 400 to 1100 nm with an average size of 620 nm (sample 6) and 580 nm (sample 7), respectively. It is clearly visible that most particles are almost perfectly spherical although some agglomerates are visible [Fig. 5(a) and (b)].

In general all physical properties of the spherical MCM-41 particles are basically identical to MCM-41 materials synthesized by well-established methods. Best results in terms of long-range order and homogeneity were achieved using the *n*-hexadecylpyridinium surfactant. In general the pore sizes of the materials prepared in homogeneous medium are a little smaller than those prepared in heterogenous systems. This confirms the results of Anderson et al. [18] who also employed a water/alcohol mixture as solvent for the prepara-

Table 2
Properties of MCM-41 spheres (homogeneous medium)

Sample No.	Template	Specific surface area[a] ($m^2 g^{-1}$)	Specific pore volume[b] (ml g^{-1})	Pore diameter $4V_p/a_s$ (nm)	Pore diameter (XRD)[c] (nm)
6	C_{16}TMABr	1100	0.78	2.84	3.14
7	C_{16}PyrCl	1220	0.95	3.14	3.05

[a] According to the BET plot.
[b] According to the Gurvitch rule.
[c] Using the d_{100}-value and assuming a pore wall thickness of 1.0 nm of sample no. 3.

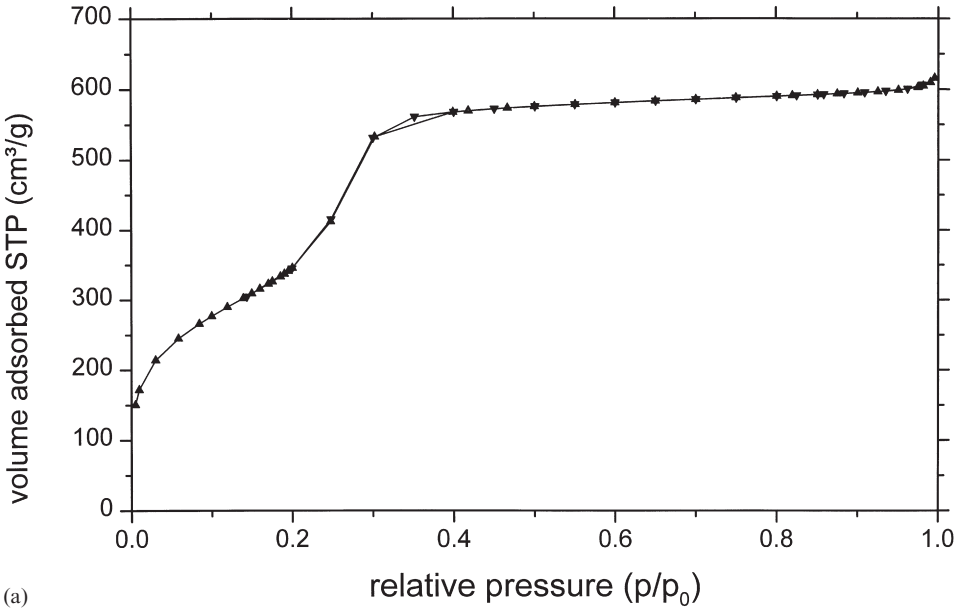

(a)

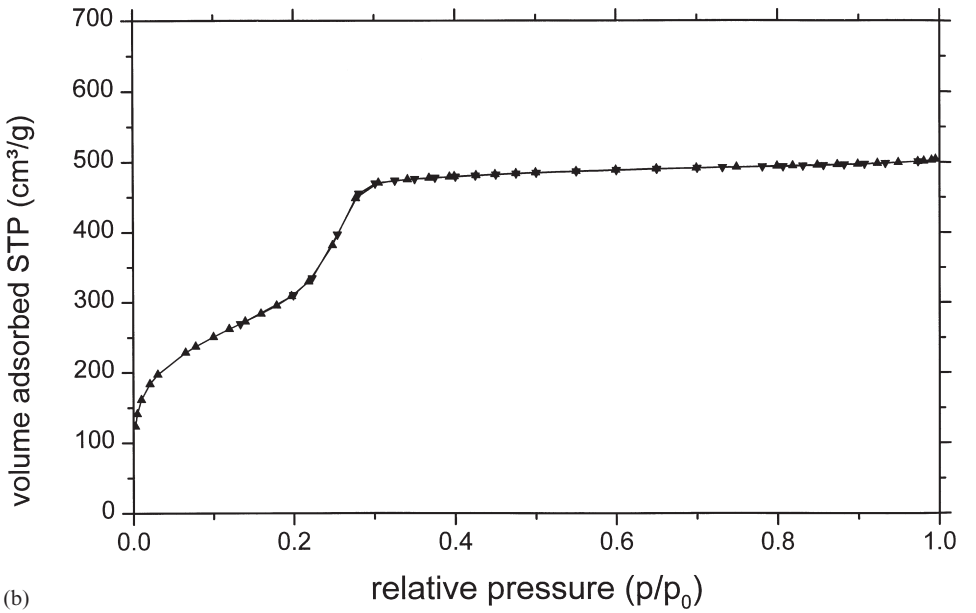

(b)

Fig. 4. (a) Nitrogen sorption isotherms of MCM-41 spheres prepared with *n*-hexadecyltrimethylammonium bromide (sample no. 6) (▲: adsorption branch, ▼: desorption branch); (b) Nitrogen sorption isotherms of MCM-41 spheres prepared with *n*-hexadecylpyridinium chloride, (sample no. 7) (▲: adsorption branch, ▼: desorption branch).

tion of mesoporous materials but used sodium hydroxide as a catalyst. According to their considerations, protonic solvents such as alcohols have the ability to reduce repulsive headgroup interactions and reduce the micelle diameters.

4.3. Aging of MCM-41 under high-pH hydrothermal conditions

Several experiments were carried out to study the behaviour of MCM-41 prepared in heterogeneous

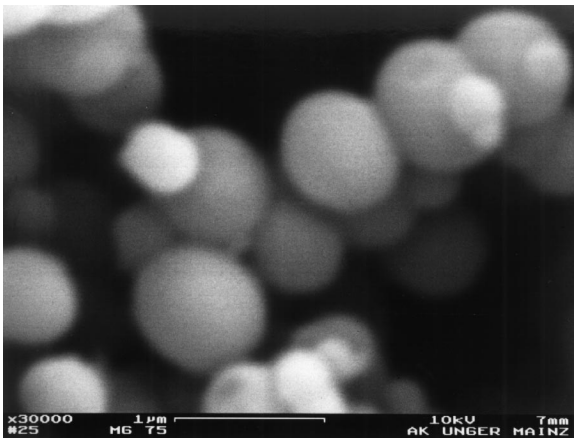

(a)

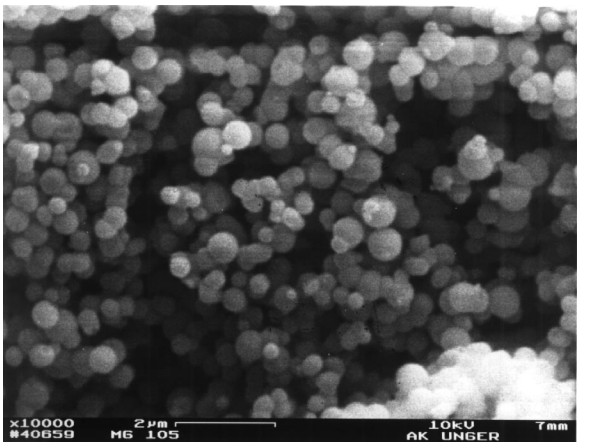

(b)

Fig. 5. (a) Scanning electron micrograph of MCM-41 spheres prepared with *n*-hexadecyltrimethylammonium bromide (sample no. 6); (b) Scanning electron micrograph of MCM-41 spheres prepared with *n*-hexadecylpyridinium chloride, (sample no. 7).

medium under high-pH conditions. Fig. 6 shows the change in the X-ray diffractograms before [Fig. 6(a)] and after [Fig. 6(b) and 6(c)] aging. The Bragg peaks in the diffractogram of the sample aged at 378 K [sample no. 9, Fig. 6(b)] apparently become sharper and an additional fifth peak can be observed at 5.70° 2θ indicating an improved long range order structure in the material.

In contrast the diffractogram of the sample aged at 433 K [sample no. 10, Fig. 6(c)] shows a broad Bragg peak at 1.14° 2Θ that could suggest the formation of another pore system while the Bragg

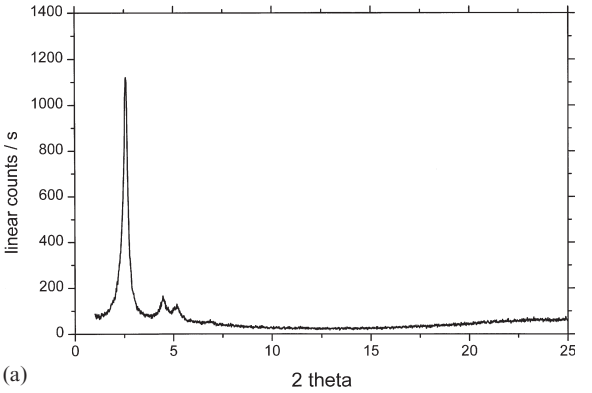

(a)

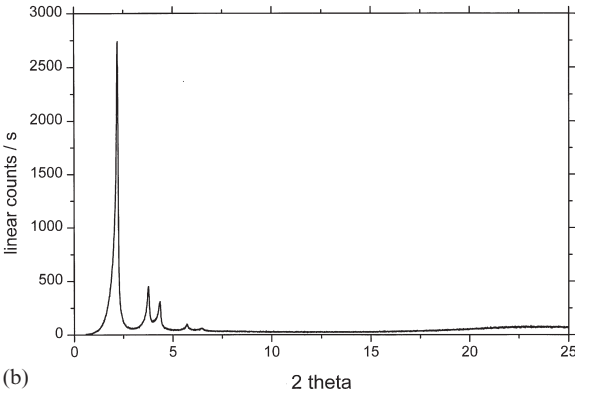

(b)

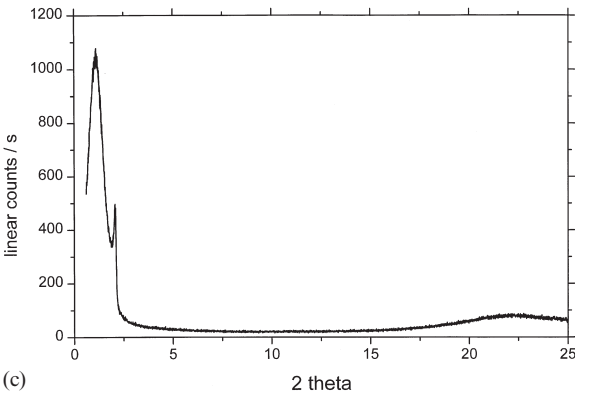

(c)

Fig. 6. (a) X-ray diffraction pattern of an untreated MCM-41 sample prepared in heterogeneous medium with *n*-hexadecyltrimethylammonium bromide as template before aging (sample no. 8); (b) X-ray diffraction pattern of a MCM-41 sample prepared in heterogeneous medium with *n*-hexadecyltrimethylammonium bromide after aging at 378 K for 10 days (sample no. 9); (c) X-ray diffraction pattern of a MCM-41 sample prepared in heterogeneous medium with *n*-hexadecyltrimethylammonium bromide after aging at 433 K for 10 days (sample no. 10).

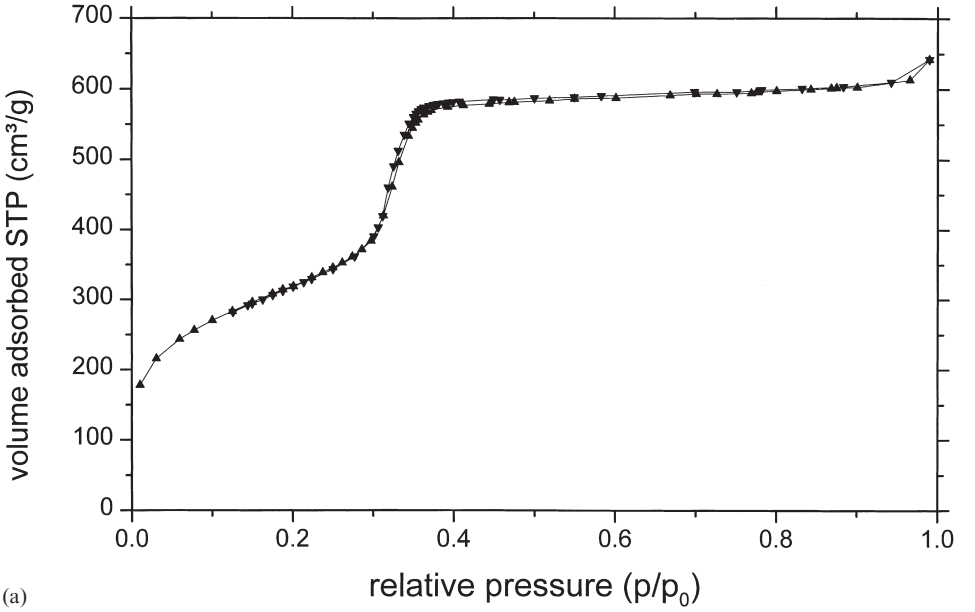

(a)

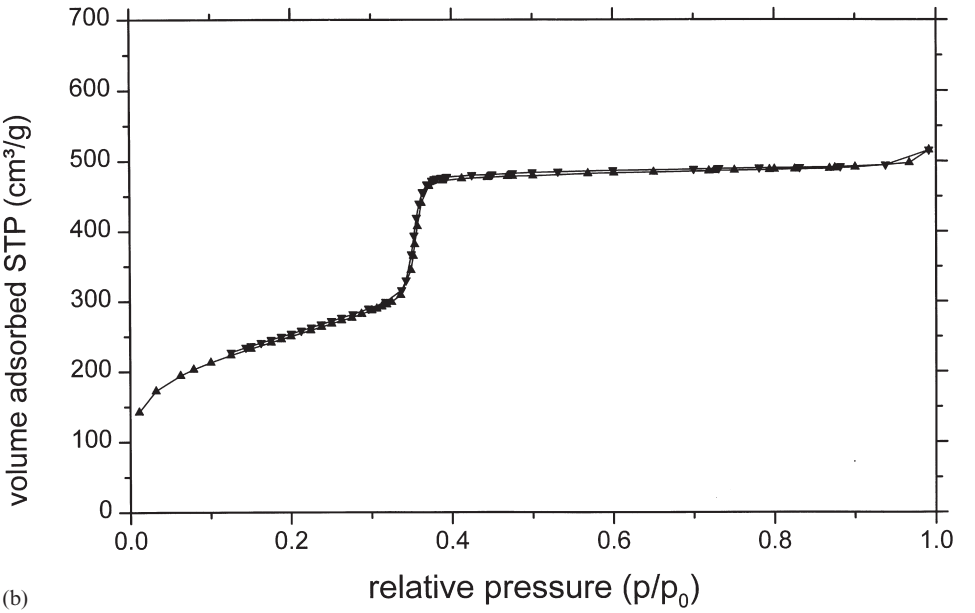

(b)

Fig. 7. (a) Nitrogen sorption isotherms of an untreated MCM-41 sample prepared with *n*-hexadecyltrimethylammonium bromide in heterogeneous medium (sample no. 8) (▲: adsorption branch, ▼: desorption branch); (b) Nitrogen sorption isotherms of an MCM-41 sample prepared with *n*-hexadecyltrimethylammonium bromide in heterogeneous medium after high-pH hydrothermal treatment at 378 K for 10 days (sample no. 9) (▲: adsorption branch, ▼: desorption branch); (c) Nitrogen sorption isotherms of an MCM-41 sample prepared with *n*-hexadecyltrimethylammonium bromide in heterogeneous medium after high-pH hydrothermal treatment at 433 K for 10 days (sample no. 10) (▲: adsorption branch, ▼: desorption branch).

peak at 2.70° 2Θ indicates that a part of the original pore arrays of 3.48 nm in diameter remain intact. These changes in X-ray diffractograms coincide with those found in pore size distributions determined by nitrogen sorption isotherms. As shown in Fig. 7, the nitrogen isotherm of the

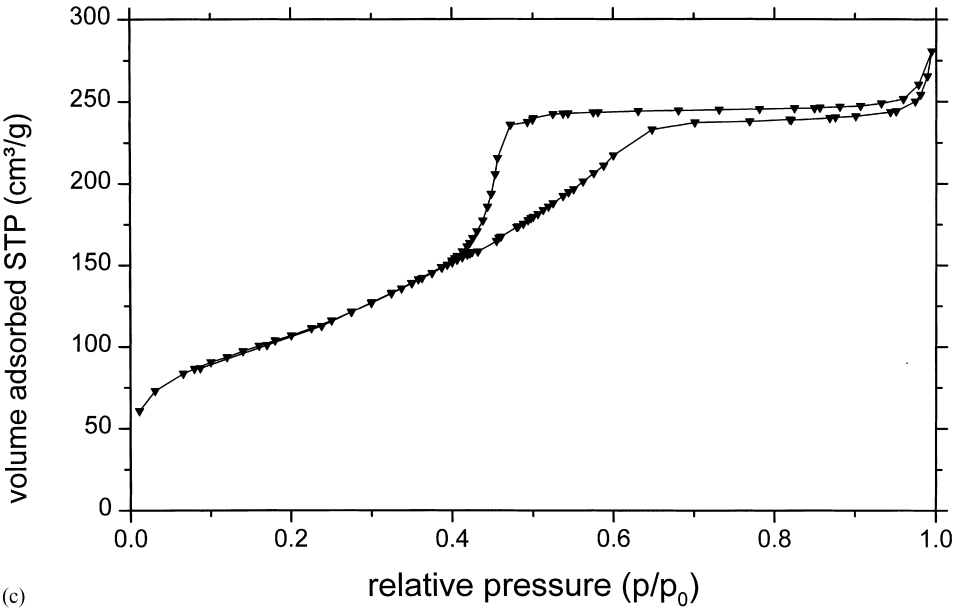

(c)

Fig. 7. (*continued*)

sample aged at 378 K [sample no. 9, Fig. 7(b)] resembles that of the untreated sample [sample no.8, Fig. 7(a)]. The increase in nitrogen uptake becomes even steeper indicating a narrower pore size distribution for this material. The sample aged at 433 K [sample no. 10, Fig. 7(c)] however shows a pronounced hysteresis loop indicating a partial disintegration of the pore structure. As shown in Table 3, the specific surface area and the specific pore volume of the sample without aging (sample no. 8) and the one aged at 378 K (sample no. 9) are comparable whereas the sample aged at 433 K (sample no. 10) shows a marked decrease of both characteristics. These results again suggest the partial collapse formation of the mesoporous structure and/or the formation of wider pores by hydrothermal after-treatment at severe conditions. Fig. 8 shows the scanning electron micrograph images of the samples before [Fig. 8(a)] and after [Fig. 8(b)] aging at 433 K. The MCM-41 particles consist of agglomerated small particles before aging that become rod-like after aging. Probably silica dissolves under these high pH-conditions and deposits at a different location. Another explanation would be the formation of holes in the pore walls.

5. Conclusion

The use of ammonia as a catalyst and tetraalkoxysilanes as silica sources provides a fast and convenient method for the preparation of high-quality MCM-41. This method has many advantages over

Table 3
Properties of hydrothermally aged MCM-41 samples

Sample no.	Aging temperature(K)	Aging time(d)	Specific surface area[a]($m^2\ g^{-1}$)	Specific pore volume[b](ml g^{-1})	Pore diameter $4V_p/a_s$(nm)
8	–	0	1142	0.99	3.48
9	378	10	895	0.80	3.56
10	433	10	387	0.39	4.00

[a] According to the BET plot.
[b] According to the Gurvitch rule.

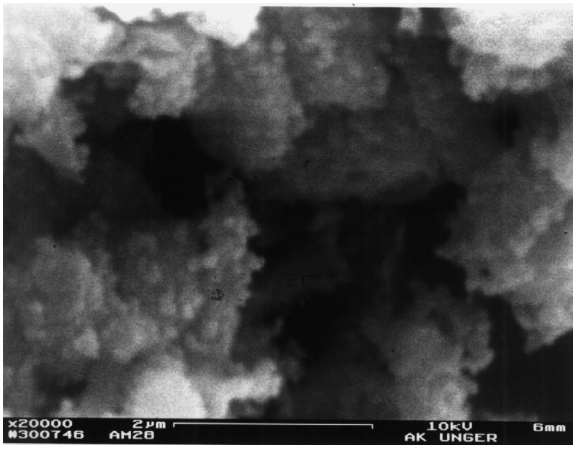

(a)

(b)

Fig. 8. (a) Scanning electron micrograph of an untreated MCM-41 sample prepared with *n*-hexadecyltrimethylammonium bromide in heterogeneous medium (sample no. 8); (b) Scanning electron micrograph of an MCM-41 sample prepared with *n*-hexadecyltrimethylammonium bromide in heterogeneous medium after high-pH hydrothermal treatment at 433 K (sample no. 10).

the common procedures and can be used both for small-scale synthesis in the laboratory and for large-scale production, which may become important if MCM-41 should be used for industrial applications. The addition of a short chain alcohol as a co-solvent allows control of the morphology during the synthesis. These spherical MCM-41 particles could be used as a starting material for spray drying to larger agglomerates which could be used for various separation techniques such as HPLC or SFC.

Acknowledgements

This work was financially supported by the Bundesministerium für Wissenschaft und Forschung through the AIF foundation (project no. 10206 N). One of the authors (A.M.) is indebted to the Ministry of Education, Science, Sports and Culture of the Japanese government for financial support of his postdoctoral research in Germany. We also thank Merck KGaA, Darmstadt, Germany for supplying chemicals and for SEM measurements. The authors would also like to thank Mr Gunter Büchel for additional SEM measurements.

References

[1] C.T. Kresge, M.E. Leonowicz, W.J. Roth, J.C. Vartuli, J.S. Beck, Nature 359 (1992) 710.
[2] J.S. Beck, J.C. Vartuli, W.J. Roth, M.E. Leonowicz, C.T. Kresge, K.D. Schmitt, C.T.-W. Chu, D.H. Olson, E.E. Sheppard, S.B. McCullen, J.B. Higgins, J.L. Schlenker, J. Am. Chem. Soc. 114 (1992) 10834.
[3] A. Corma, M.T. Navarro, J.P. Pariente, J. Chem. Soc., Chem. Commun. (1994) 147.
[4] P.T. Tanev, M. Chibwe, T.J. Pinnavaia, Nature 368 (1994) 321.
[5] A. Corma, V. Fornes, M.T. Navarro, J.P. Pariente, J. Catal. 148 (1994) 569.
[6] R. Schmidt, M. Stöcker, E. Hansen, D. Akporiaye, O.H. Ellestad, Microporous Mater. 3 (1995) 443.
[7] P.J. Branton, P.G. Hall, K.S.W. Sing, J. Chem. Soc., Chem. Commun. (1993) 1257.
[8] Q. Huo, D.I. Margolese, U. Ciesla, D.G. Demuth, P. Feng, T.E. Gier, P. Sieger, A. Firouzi, B.F. Chmelka, F. Schüth, G.D. Stucky, Chem. Mater. 6 (1994) 1176.
[9] D.M. Antonelli, J.Y. Ying, Angew. Chem., Int. Ed. Engl. 18 (1995) 34.
[10] M. Grün, A.A. Kurganov, S. Schacht, F. Schüth, K.K. Unger, J. Chromatogr. A 740 (1996) 1.
[11] M. Grün, I. Lauer, K.K. Unger, Adv. Mat. 9 (1997) 254.
[12] K. Schumacher, M. Grün, N. v. Döhren, K.K. Unger, poster presentation, 2nd SFC User Meeting, Siegen, October 1997.
[13] W. Stöber, A. Fink, E. Bohn, J. Colloid Interface Sci. 26 (1968) 62.
[14] P.I. Ravikovitch, D. Wie, W.T. Chueh, G.L. Haller, A.V. Neimark, J. Phys. Chem. B. 101 (1997) 3673.
[15] A.V. Neimark, P.I. Ravikovitch, M. Grün, F. Schüth, K.K. Unger, COPS-IV Symposium, Bath, oral presentations, 1996.
[16] P.I. Ravikovitch, S.C. Ó Domhnaill, A.V. Neimark, F. Schüth, K.K. Unger, Langmuir 11 (1995) 4765.
[17] E.L. Colichman, J. Am. Chem. Soc. 72 (1950) 1834.
[18] M.T. Anderson, J.E. Martin, J.G. Odinek, P.P. Newcomer, Chem. Mater. 10 (1998) 311.